A

Adenocarcinoma						
	Total case no.	+++	++	+	—	Positive (%)
HPC1	27	0	6	13	8	70.37
HPC2		1	2	9	15	44.44
HPC4		5	18	2	2	92.59
Con phage		0	0	0	27	0.00
Papillary adenocarcinoma						
	Total case no.	+++	++	+	—	Positive (%)
HPC1	8	2	1	3	2	75.00
HPC2		0	1	3	4	50.00
HPC4		1	5	1	1	87.50
Con phage		0	0	0	8	0.00
Bronchioloalveolar carcinoma						
	Total case no.	+++	++	+	—	Positive (%)
HPC1	8	2	4	1	1	87.50
HPC2		0	0	1	7	12.50
HPC4		1	5	1	1	87.50
Con phage		0	0	0	8	0.00
Squamous cell carcinoma						
	Total case no.	+++	++	+	—	Positive (%)
HPC1	27	5	7	12	3	88.89
HPC2		0	2	7	18	33.33
HPC4		9	16	1	1	96.30
Con phage		0	0	0	27	0.00
Large cell carcinoma						
	Total case no.	+++	++	+	—	Positive (%)
HPC1	10	0	6	3	1	90.00
HPC2		0	0	4	6	40.00
HPC4		5	4	0	1	90.00
Con phage		0	0	0	10	0.00
Small cell carcinoma						
	Total case no.	+++	++	+	—	Positive (%)
HPC1	8	2	5	1	0	100.00
HPC2		0	0	2	6	25.00
HPC4		5	3	0	0	100.00
Con phage		0	0	0	8	0.00

B

Metastatic adenocarcinoma from lung						
	Total case no.	**+++**	**++**	**+**	**—**	**Positive (%)**
HPC1	8	0	1	6	1	87.50
HPC2		0	0	3	5	37.50
HPC4		2	4	2	0	100.00
Con phage		0	0	0	8	0.00
Metastatic squamous cell carcinoma from lung						
	Total case no.	**+++**	**++**	**+**	**—**	**Positive (%)**
HPC1	4	0	2	0	2	50.00
HPC2		0	0	1	3	25.00
HPC4		2	2	0	0	100.00
Con phage		0	0	0	4	0.00

C

Normal pneumonic tissue						
	Total case no.	**+++**	**++**	**+**	**—**	**Positive (%)**
HPC1	6	0	0	0	6	0.00
HPC2		0	0	0	6	0.00
HPC4		0	0	0	6	0.00
Con phage		0	0	0	6	0.00
Cancer adjacent normal pneumonic tissue						
	Total case no.	**+++**	**++**	**+**	**—**	**Positive (%)**
HPC1	6	0	0	0	6	0.00
HPC2		0	0	0	6	0.00
HPC4		0	0	0	6	0.00
Con phage		0	0	0	6	0.00

Table S1. Clinical response rates in human lung cancer surgical specimens, as evidenced by immunohistochemistry (IHC) using HPC1, HPC2, and HPC4.

(A) Several histopathological subtypes of clinical human lung cancer biopsies were immunostained by HPC1, HPC2, or HPC4, and compared to control phage. The positive response percentages were calculated and compiled. (B) IHC data for metastatic adenocarcinoma and SCC from lung. (C) Tumor specific binding of HPC1, HPC2, and HPC4 were examined using normal pneumonic tissue and cancer adjacent normal pneumonic tissue. Reaction area: +++, >50%; ++, 50~20%; +, <20%; －, 0%.

A

Adenocarcinoma

	Grade	Stage	Type	Con phage	HPC1	HPC2	HPC4
AD1	1	T2N1M0	Malignant	–	++	–	+++
AD2	1	T2N1M0	Malignant	–	+	–	++
AD3	1	T4NxM0	Malignant	–	–	+	+
AD4	2	T2N1M0	Malignant	–	++	+	+++
AD5	2	T1N0M0	Malignant	–	++	+	++
AD6	-	T1N0M0	Malignant	–	+	–	+++
AD7	1	T3N1M0	Malignant	–	+	+	++
AD8	2	T1NxM0	Malignant	–	+	–	++
AD9	1	TxN0M0	Malignant	–	+	–	++
AD10	1	T4N1M0	Malignant	–	+	+	++
AD11	1	T1NxM0	Malignant	–	–	–	++
AD12	2	T4N2M0	Malignant	–	–	+	++
AD13	2	T3N1M0	Malignant	–	–	–	–
AD14	2	T3N1M0	Malignant	–	–	–	–
AD15	2	T3N1M1	Malignant	–	–	–	++
AD16	3	T2N0M0	Malignant	–	+	++	++
AD17	2	T2N0M1	Malignant	–	+	+++	++
AD18	2	T2N0M0	Malignant	–	++	–	++
AD19	2	T2N0M0	Malignant	–	+	++	+++
AD20	2	T2N1M0	Malignant	–	–	+	++
AD21	3	T4NxM0	Malignant	–	+	–	++
AD22	2	T3N0M0	Malignant	–	+	+	++
AD23	3	T4N0M0	Malignant	–	++	+	+++
AD24	3	T3N0M0	Malignant	–	–	–	++
AD25	3	T1N0M0	Malignant	–	++	–	++
AD26	3	T2N0M0	Malignant	–	+	–	++
AD27	3	T2N0M0	Malignant	–	+	–	+

B

Papillary adenocarcinoma

	Grade	Stage	Type	Con phage	HPC1	HPC2	HPC4
PAD1	1	T3N0M0	Malignant	–	+	+	++
PAD2	1	T2NxM0	Malignant	–	+	++	+++
PAD3	2	T1N0M0	Malignant	–	–	+	++
PAD4	2	T2N0M0	Malignant	–	+	+	++
PAD5	1	T1N0M0	Malignant	–	–	–	–
PAD6	2	T1N0M0	Malignant	–	+++	–	++
PAD7	2 - 3	TxNxMx	Malignant	–	++	–	+
PAD8	2	T2N0M0	Malignant	–	+++	–	++

C

Bronchioloalveolar carcinoma

	Grade	Stage	Type	Con phage	HPC1	HPC2	HPC4
BAC1	-	T2N0M0	Malignant	–	++	–	++
BAC2	-	T3N0M0	Malignant	–	++	–	++
BAC3	-	T2N0M0	Malignant	–	+	–	++
BAC4	-	T2N0M0	Malignant	–	+++	+	++
BAC5	-	T2N0M0	Malignant	–	++	–	+
BAC6	-	T1N0M0	Malignant	–	++	–	+++
BAC7	-	T2N0M0	Malignant	–	–	–	–
BAC8	-	TxNxMx	Malignant	–	+++	–	++

D

Squamous cell carcinoma

	Grade	Stage	Type	Con phage	HPC1	HPC2	HPC4
SCC1	1	T2N0M0	Malignant	–	++	+	+++
SCC2	1	T1NxM0	Malignant	–	+	–	++
SCC3	1	T2N1M0	Malignant	–	+	++	++
SCC4	1	T2N3M0	Malignant	–	+	+	++
SCC5	1	T3N1M0	Malignant	–	++	+	+++
SCC6	1	T2N1M0	Malignant	–	+	–	++
SCC7	1	T2N1M0	Malignant	–	++	+	+++
SCC8	1	T2NxM0	Malignant	–	++	–	+++
SCC9	1	T2N0M0	Malignant	–	+	–	+++
SCC10	1	T4NxM1	Malignant	–	–	–	–
SCC11	1	T3N1M0	Malignant	–	++	–	++
SCC12	2	T3N0M0	Malignant	–	+++	+	++
SCC13	1	T3N1M0	Malignant	–	+	++	+++
SCC14	2	T2N0M0	Malignant	–	+	–	++
SCC15	2	T2N0M0	Malignant	–	+	–	++
SCC16	2	T2N1M0	Malignant	–	–	–	+
SCC17	2	T3N3M0	Malignant	–	+	+	++
SCC18	3	T2N0M0	Malignant	–	+	–	++
SCC19	2	T3N1M0	Malignant	–	+	–	++
SCC20	2	T1N0M0	Malignant	–	+++	–	++
SCC21	3	T3NxM0	Malignant	–	+++	–	++
SCC22	3	T1N0M0	Malignant	–	++	–	+++
SCC23	3	T2N0M0	Malignant	–	++	–	+++
SCC24	3	T2N0M0	Malignant	–	+++	–	+++
SCC25	3	T3N3M0	Malignant	–	+	–	++
SCC26	3	T3N1M0	Malignant	–	–	+	++
SCC27	3	T2N0M0	Malignant	–	+++	–	++

E

Large cell carcinoma

	Grade	Stage	Type	Con phage	HPC1	HPC2	HPC4
GCC1	-	T2N0M0	Malignant	–	++	+	+++
GCC2	-	T3N0M0	Malignant	–	++	+	+++
LCC1	-	T3N0M0	Malignant	–	++	–	++
LCC2	-	T2NxM0	Malignant	–	++	+	+++
LCC3	-	T3N1M0	Malignant	–	+	–	++
LCC4	-	T2NxM0	Malignant	–	+	–	++
LCC5	-	T3NxM0	Malignant	–	++	+	+++
LCC6	-	T3N1M0	Malignant	–	+	–	++
LCC7	-	T2N0M0	Malignant	–	++	–	+++
LCC8	-	T3NxM0	Malignant	–	–	–	–

F

Small cell carcinoma

	Grade	Stage	Type	Con phage	HPC1	HPC2	HPC4
SmCC1	-	T3N1M0	Malignant	–	+++	–	+++
SmCC2	-	T3N2M0	Malignant	–	+	–	++
SmCC3	-	T2N1M0	Malignant	–	++	–	+++
SmCC4	-	T3NxM0	Malignant	–	++	–	+++
SmCC5	-	T2N1M0	Malignant	–	++	–	+++
SmCC6	-	T3N0M0	Malignant	–	++	+	+++
SmCC7	-	T2N0M0	Malignant	–	++	–	++
SmCC8	-	T2N0M0	Malignant	–	+++	+	++

Table S2. Pathological diagnostic information of lung cancer stage and grade and their correlation to HPC1, HPC2, and HPC4 response rates.

Reaction area: +++, >50%; ++, 50~20%; +, <20%; －, 0%.

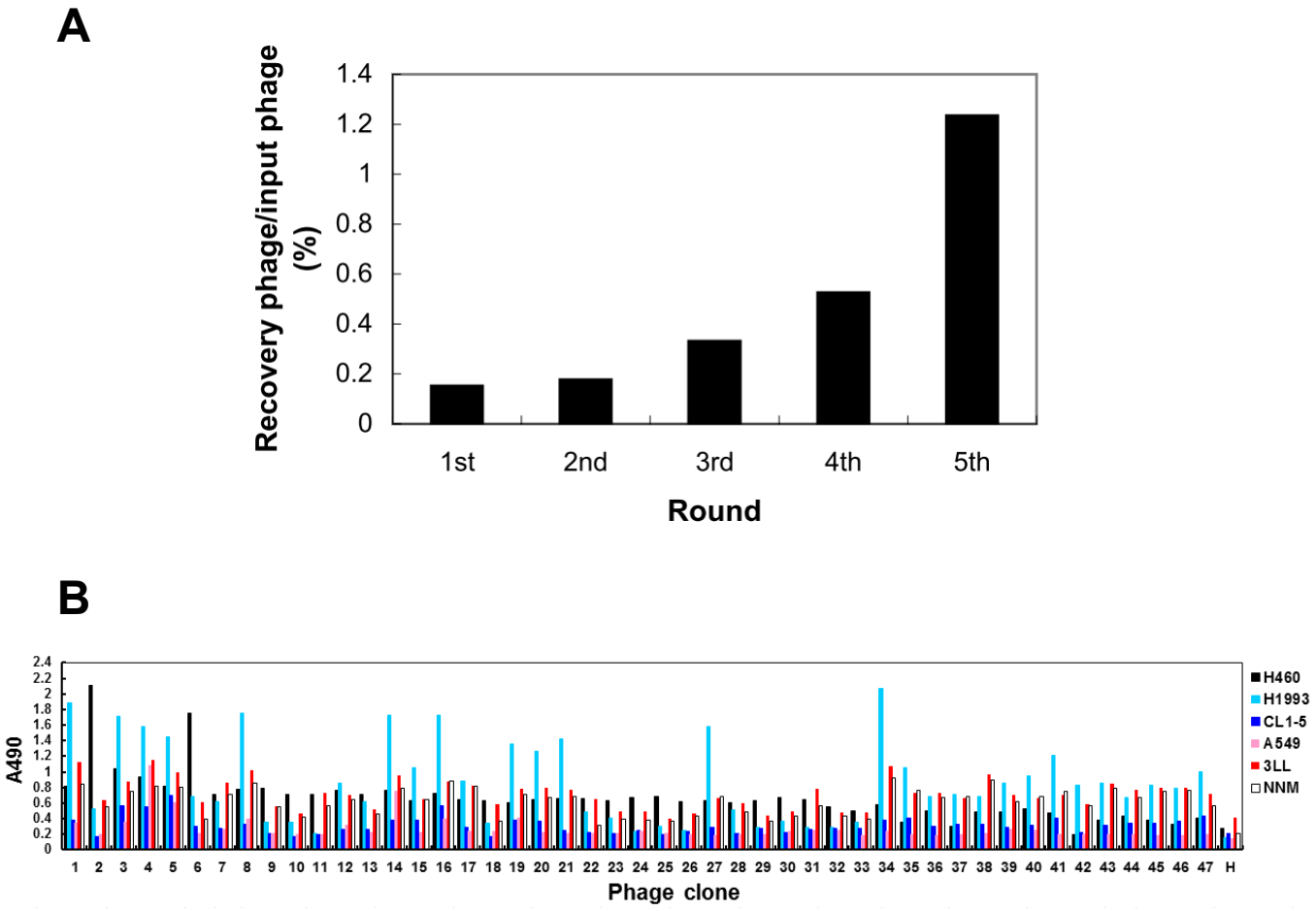

Figure S1. *In vitro* phage display biopanning and selection of phage clones that bind to NSCLC cell lines.

(A) A phage displayed random peptide library was used to select phages that bind to the lung large cell carcinoma cell line H460. (B) Forty-seven H460 bound phage clones with higher binding ability to NCI-H1993, CL1-5, A549, and 3LL cell lines were selected from the fifth round of biopanning for ELISA screening. Helper phage was used as a negative control. NNM was used as the normal cell control.

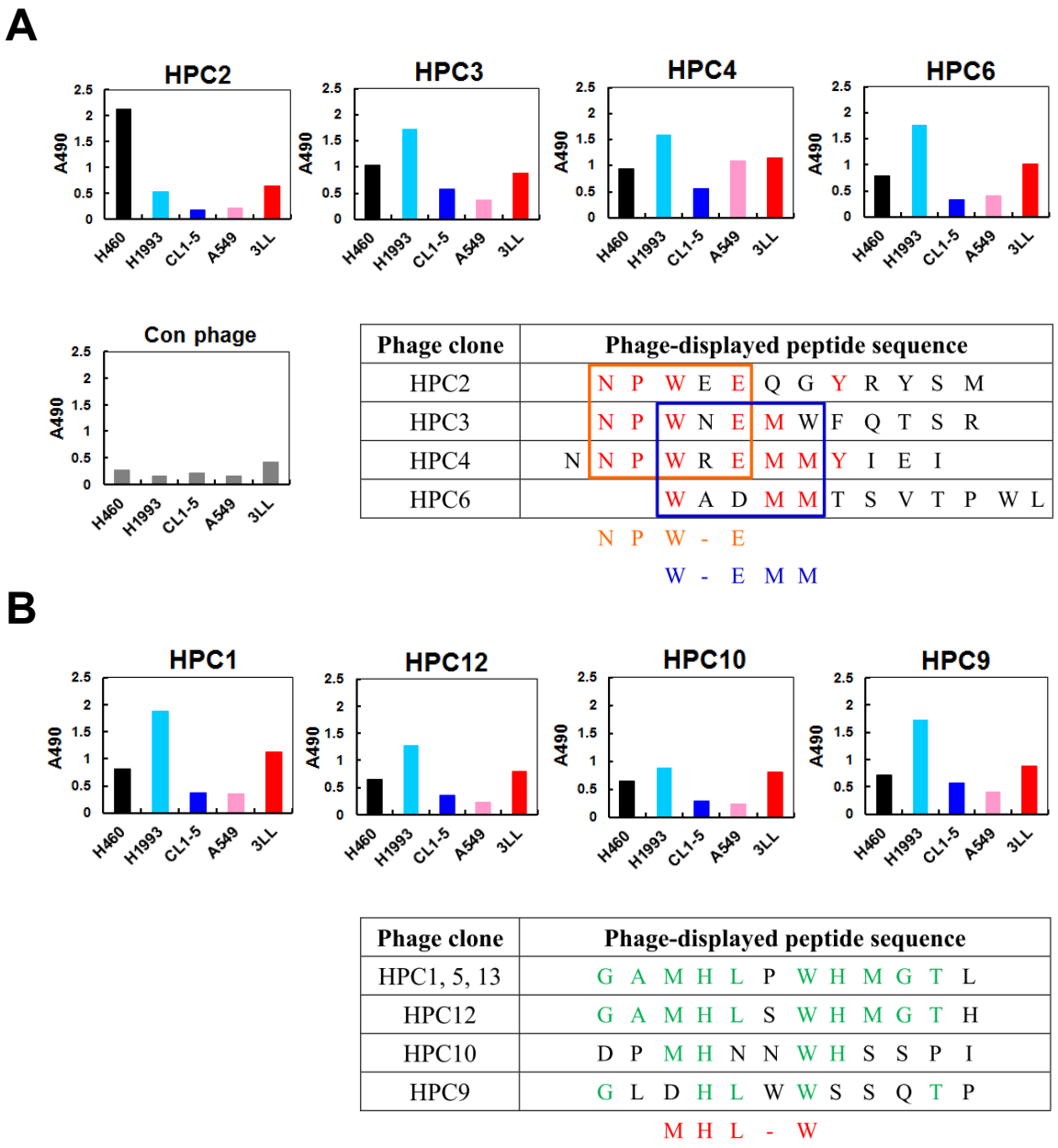

Figure S2. Predicted motifs and lung cancer cell line binding patterns of two major phage clone groups.

(A) Binding intensity of HPC2, HPC3, HPC4, and HPC6 to H460, H1993, CL1-5, A549, and 3LL, as measured by ELISA of paraformaldehyde-fixed cells. The binding patterns of HPC3, HPC4, and HPC6 to these cell lines are similar, and distinct from those of HPC2. These data, combined with the observation that HPC4 exhibits better response rates in clinical biopsy and other cell-level experiments, suggest that the W-EMM mimetic motif plays a more important role than the NPW motif in human lung cancer binding. (B) HPC1, HPC12, HPC10, and HPC9 show similar binding patterns, suggesting that the MHL-W consensus sequence contributes to such binding.

A

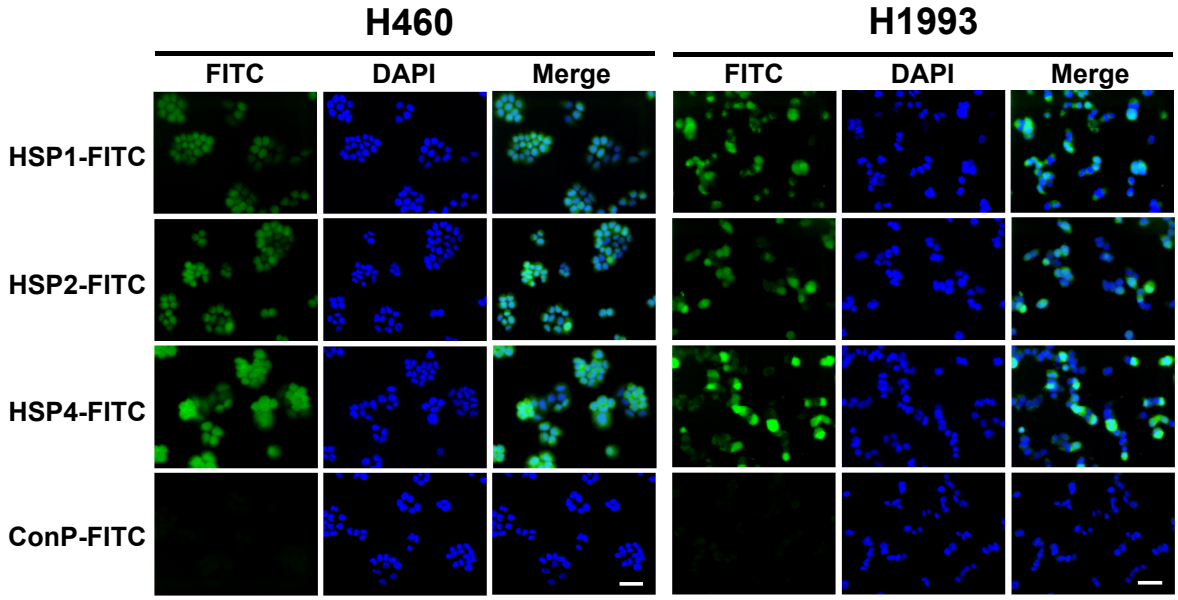

B

IFA Positive Cells (%)			
	HSP1-FITC	HSP2-FITC	HSP4-FITC
H460	77.01 %	76.5 %	83.22%
H1993	66.94 %	61.11 %	55.93%

Figure S3. Determination of binding specificity of FITC-labeled HSP1, HSP2, and HSP4 peptides to H460 and H1993 cells by immunofluorescent staining.

(A) Immunofluorescent staining of FITC-labeled HSP1, HSP2, and HSP4 peptides to H460 large cell carcinoma and H1993 adenocarcinoma cell lines. Nuclei were stained with DAPI. Scale bar, 50 μm. (B) Table listing the percentage of IFA-positive cells for HSP1, HSP2, and HSP4-FITC in H460 and H1993 cell lines.

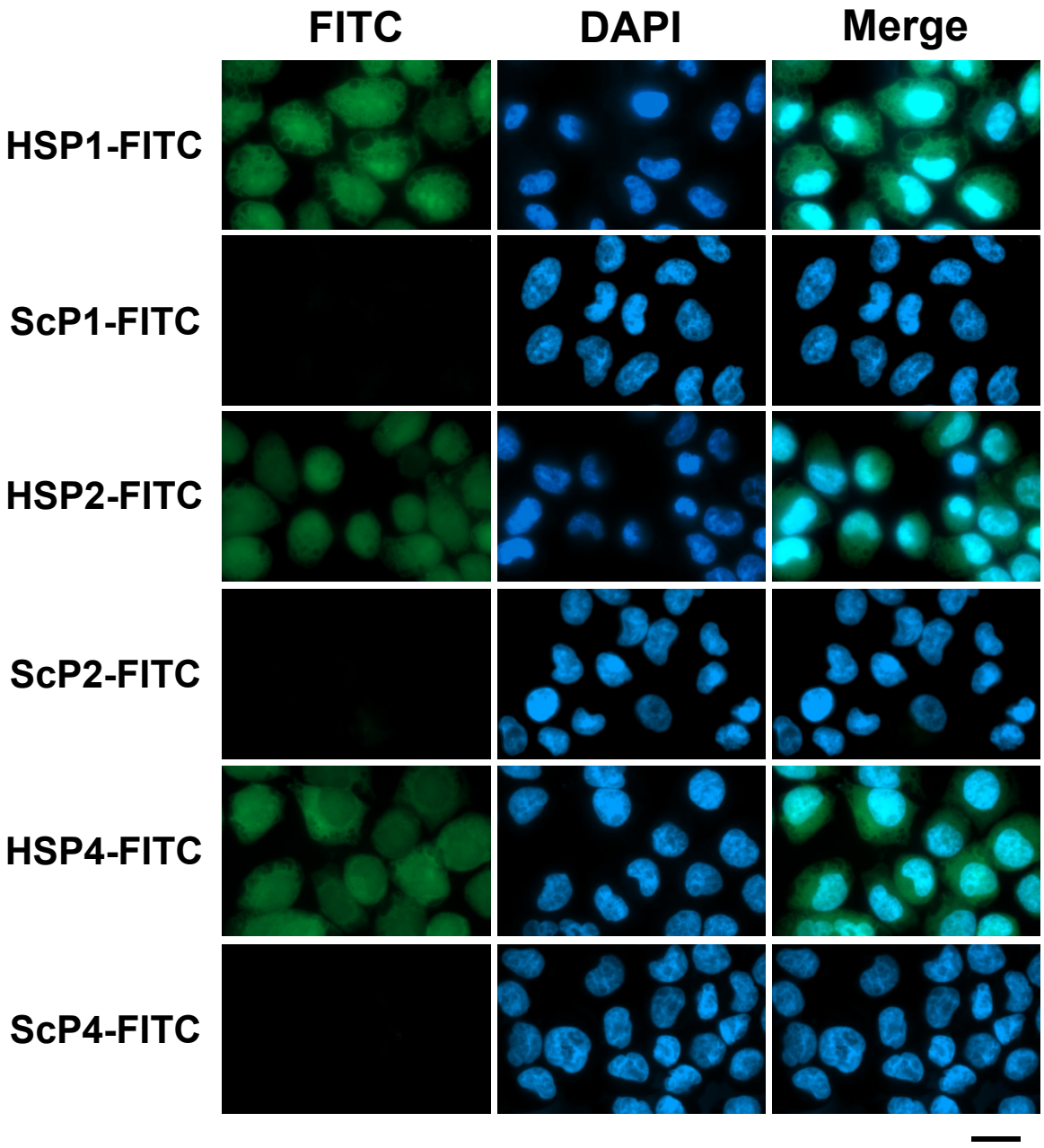

Figure S4. Scrambled peptides show no binding ability to H460 cells.

Immunofluorescent staining of FITC-labeled scrambled peptides ScP1 (LGHPMATMWLGH), ScP2 (MYQEPSRWGENY), and ScP4 (IMEWNEYIMRPN) corresponding to HSP1, HSP2, and HSP4 for H460 binding. The nuclei were stained with DAPI. Scale bar, 20 μm.

Figure S5.

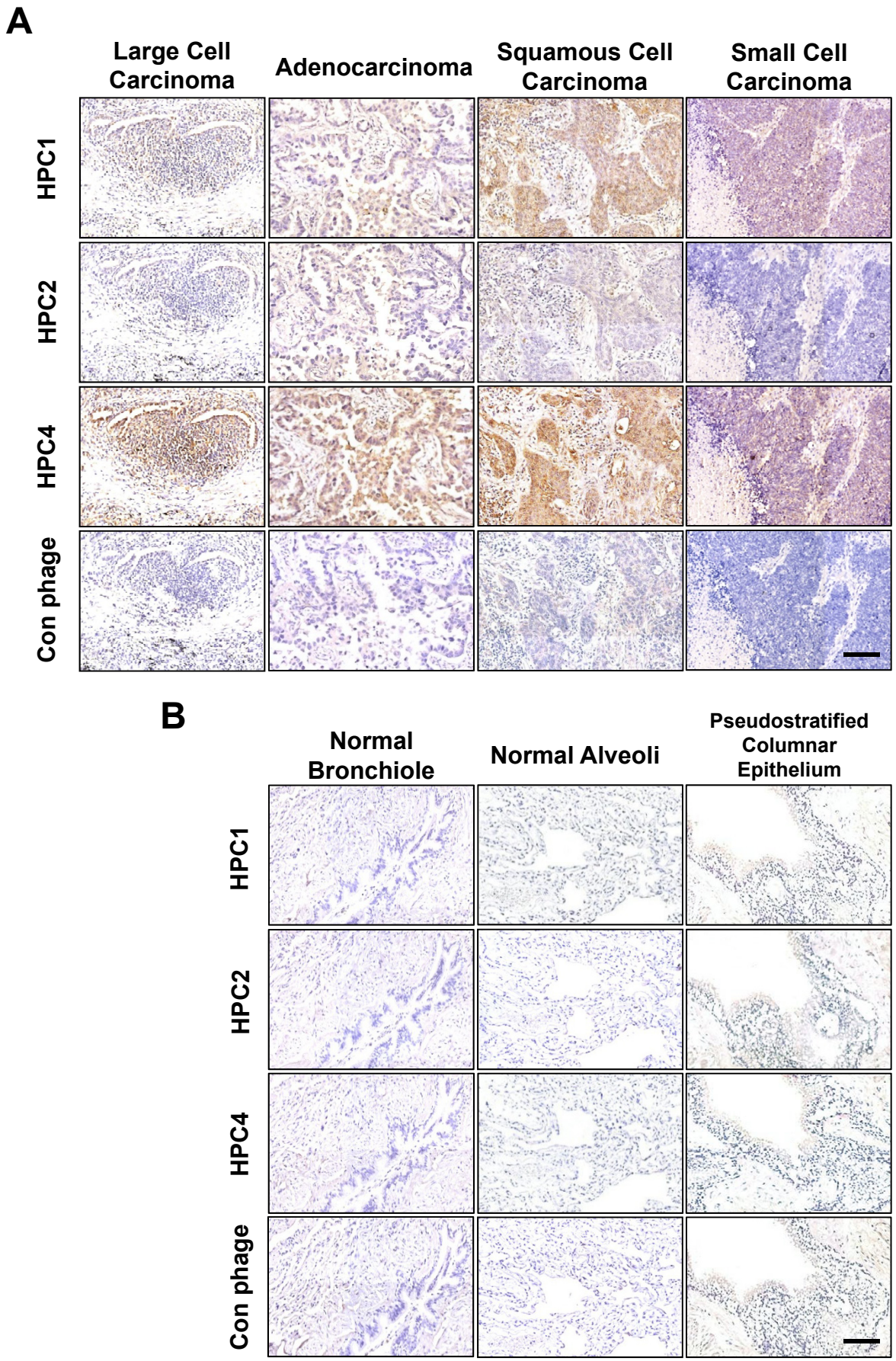
A
Large Cell Carcinoma
Adenocarcinoma
Squamous Cell Carcinoma
Small Cell Carcinoma
HPC1
HPC2
HPC4
Con phage
B
Normal Bronchiole
Normal Alveoli
Pseudostratified Columnar Epithelium
HPC1
HPC2
HPC4
Con phage

Figure S5. Immunohistochemical staining of human NSCLC, SCLC, and normal pneumonic tissues with HPC1, HPC2, and HPC4.

Lower magnification (larger field of view) images, comparable to those shown in Figure 1B. (A) Serial sections of four subtypes of NSCLC and SCLC revealed prominent staining in tumor regions by HPC1 and HPC4, but weak or no signals in stroma regions. (B) Three histological types of tissue in normal lung did not cross-react with HPC1, HPC2, or HPC4. The same phage titer ($2\sim5 \times 10^8$ pfu/μl) was used in each type of tissue. Helper phage was used as a negative control. Scale bar, 100 μm.

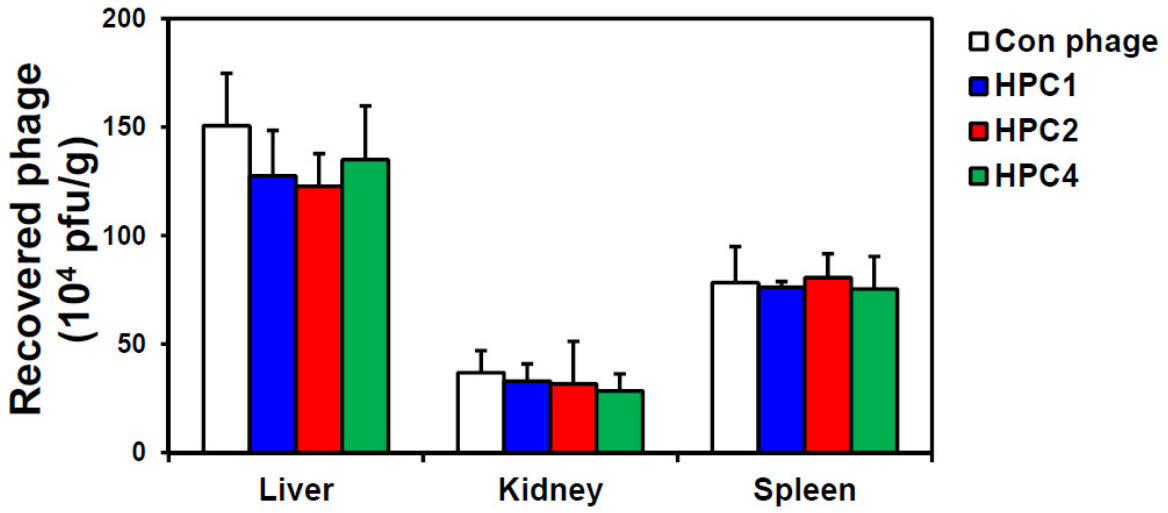

Figure S6. Phage distribution of the liver, kidney, and spleen in tumor-homing experiments.

Although there was a noticeable uptake of phage by the organs of mononuclear phagocyte system such as the liver and spleen, no significant difference in accumulation between the targeting and control phages was observed in these organs.

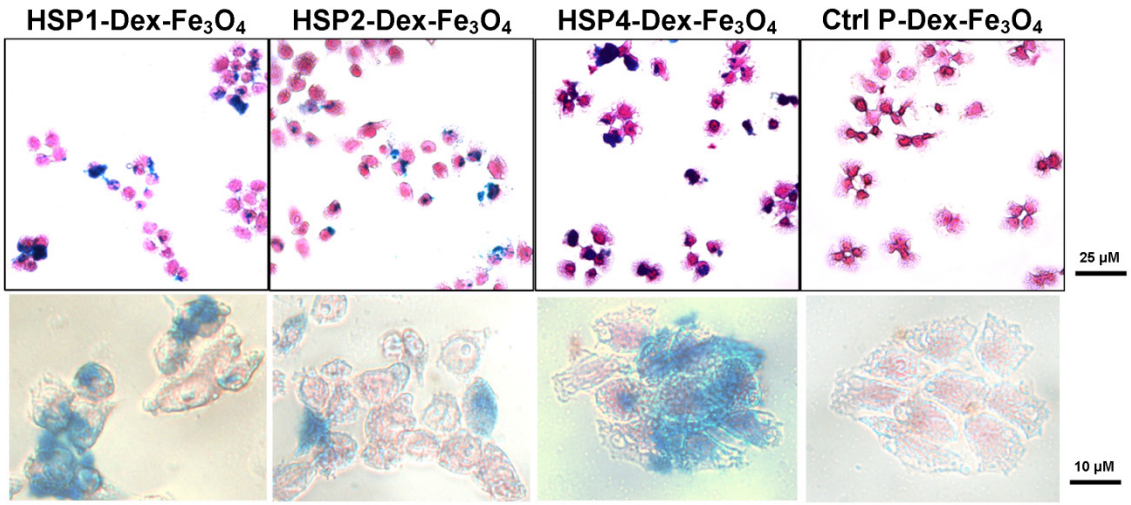

Figure S7. *In vitro* cell binding of targeting SPIONs.

Prussian blue staining of fixed H460 cells treated with HSP1-, HSP2-, HSP4-, Ctrl P-Dex-Fe_3O_4, or Dex-Fe_3O_4 nanoparticles (10 μg/ml) for 1 hr.

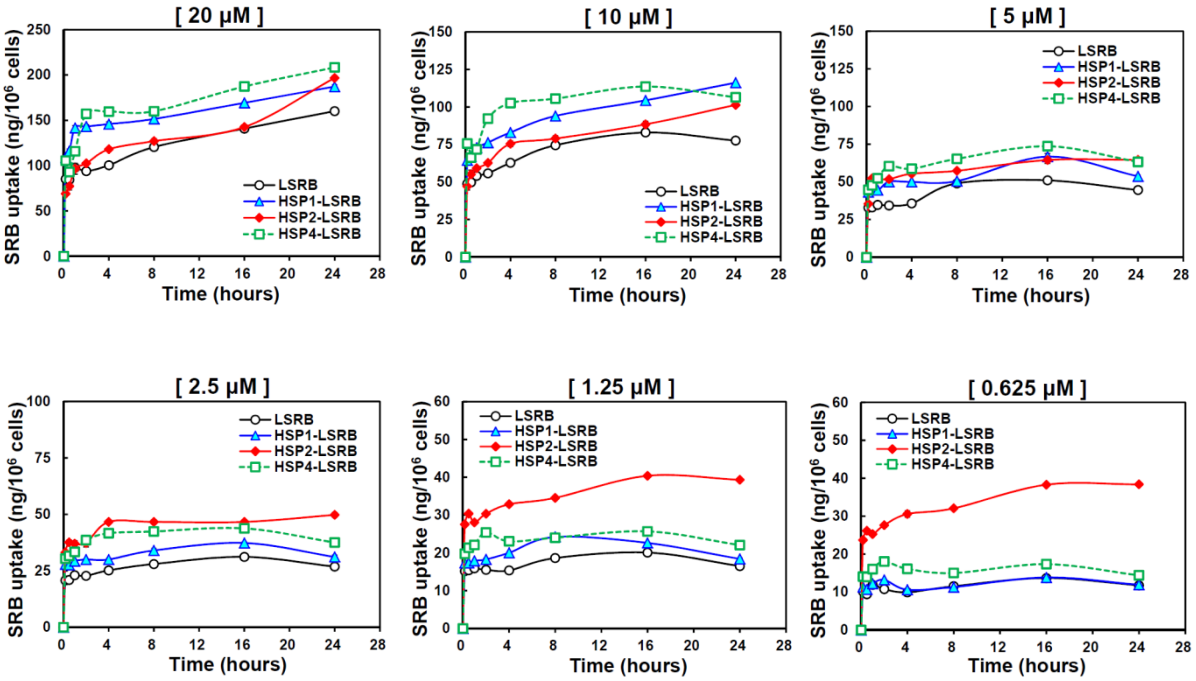

Figure S8. HSP1, HSP2, and HSP4 peptides enhance LSRB in a human lung cancer cell line, H460.

Kinetics of HSP1-LSRB, HSP2-LSRB, HSP4-LSRB, and LSRB uptake by H460 cells at 37˚C. After washing with acid glycine buffer to remove surface-bound liposomal dye, internalized SRB was quantified (n=4).

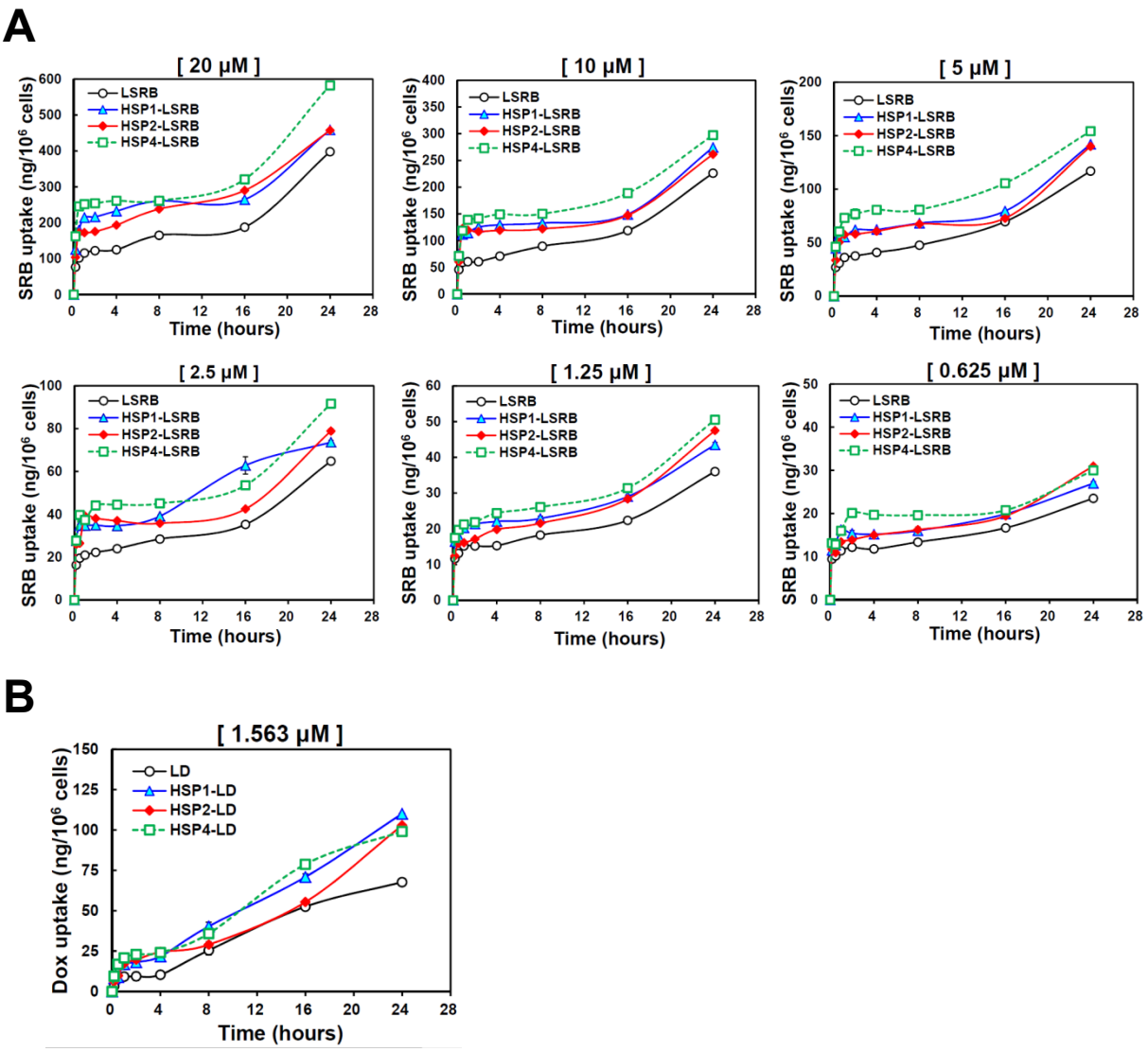

Figure S9. HSP1, HSP2, and HSP4 peptides enhance LSRB internalization and LD uptake in a human lung adenocarcinoma cell line, H1993.

(A) Uptake kinetics of non-targeting LSRB and peptide (HSP1, HSP2, and HSP4)-conjugated LSRB by H1993 cells at 37°C. After washing with acid glycine buffer to remove surface-bound liposomal dye, internalized SRB was quantified (n=4). These results indicate that HSP4 is most effective at triggering endocytosis in the H1993 adenocarcinoma cell line from low to high concentrations; notably, this kinetic pattern is distinct from that observed using H460 large cell carcinoma cell lines (Figure S8). (B) LD uptake by cells can be observed at a low drug concentration which is insufficient to cause cell death. The kinetics of HSP1-, HSP2-, and HSP4-LD uptake by H1993 cells at a doxorubicin concentration of 1.563 μM were generally compatible with the LSRB uptake data (panel A), indicating that HSP4 is efficacious at LD uptake.

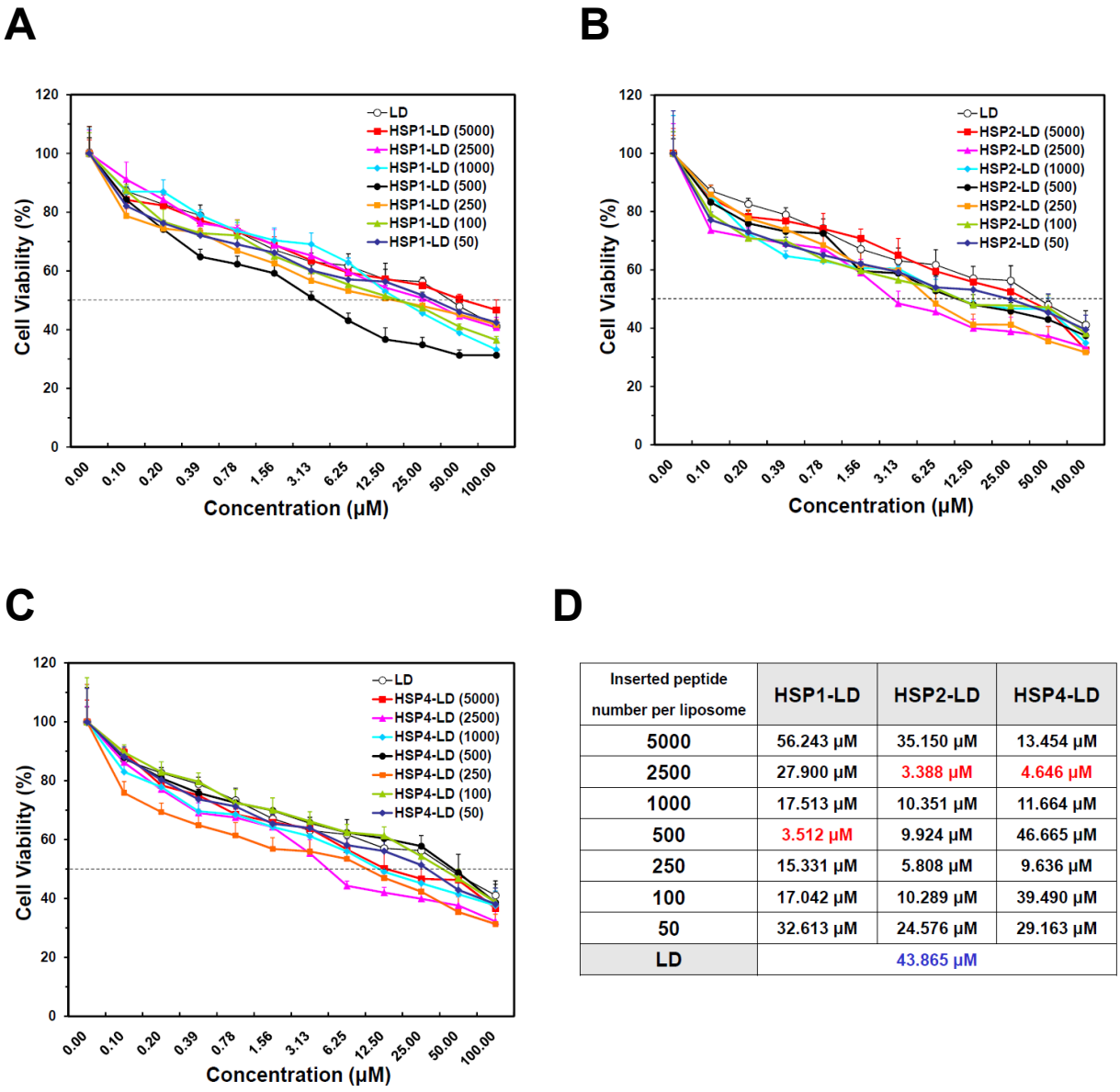

Inserted peptide number per liposome	HSP1-LD	HSP2-LD	HSP4-LD
5000	56.243 μM	35.150 μM	13.454 μM
2500	27.900 μM	3.388 μM	4.646 μM
1000	17.513 μM	10.351 μM	11.664 μM
500	3.512 μM	9.924 μM	46.665 μM
250	15.331 μM	5.808 μM	9.636 μM
100	17.042 μM	10.289 μM	39.490 μM
50	32.613 μM	24.576 μM	29.163 μM
LD	43.865 μM		

Figure S10. Different numbers of peptide inserted into a liposome have different cytotoxic effects on cancer cells.

H460 cells were treated with varying numbers (50, 100, 250, 500, 1000, 2500, or 5000) of peptides inserted into drug liposomes, and living cells were measured by MTT assay. Peptide numbers required for greatest efficacy differed with peptide. (A) HSP1, (B) HSP2, and (C) HSP4 (n=6). (D) Table comparing the IC_{50} values of different insert numbers for each peptide. The numbers resulting in greatest efficacy for HSP1, HSP2, and HSP4 were 500, 2500, and 2500 peptides per liposome, respectively.

Figure S11.

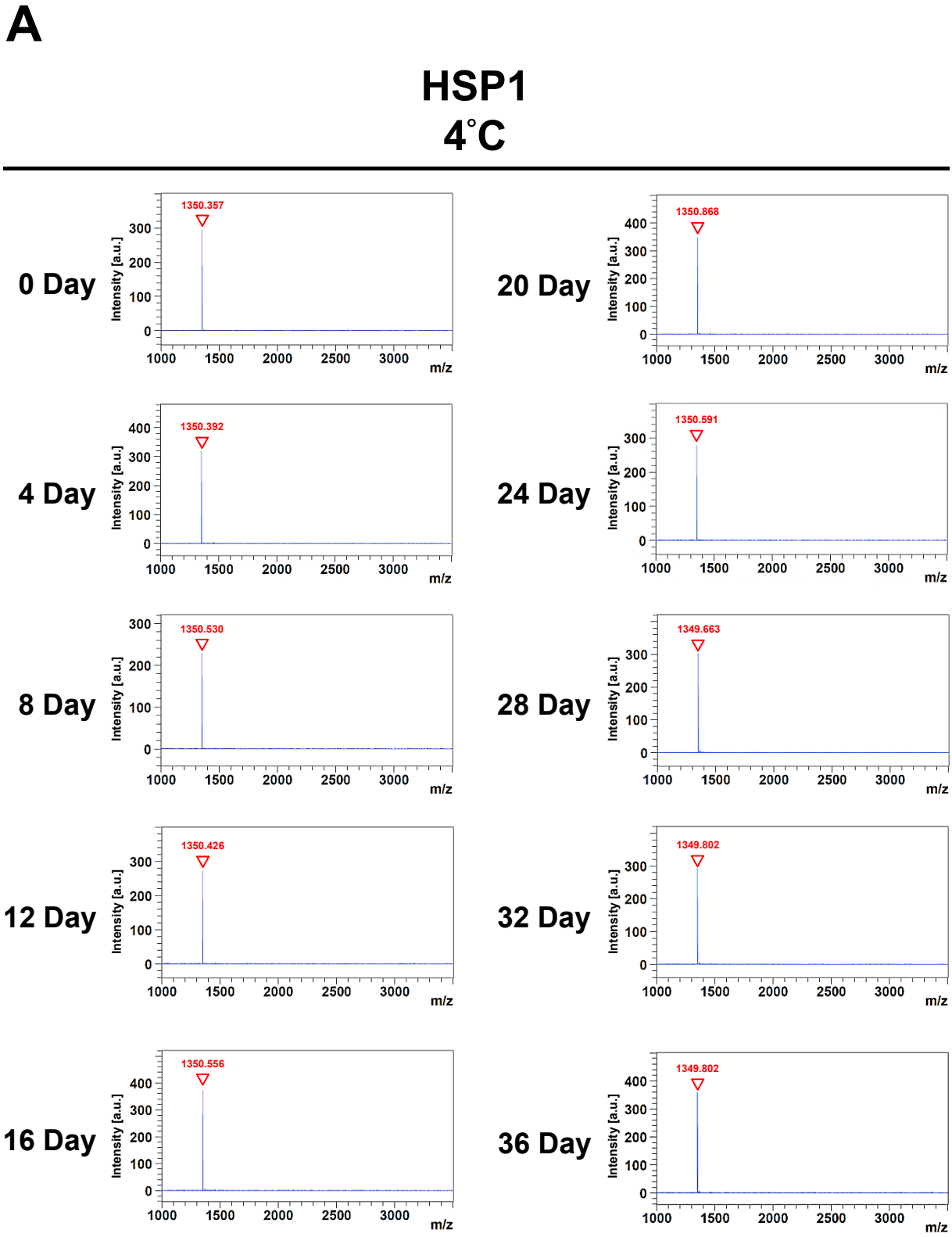
A
HSP1
4°C
0 Day
1350.357
20 Day
1350.868
4 Day
1350.392
24 Day
1350.591
8 Day
1350.530
28 Day
1349.663
12 Day
1350.426
32 Day
1349.802
16 Day
1350.556
36 Day
1349.802
Intensity [a.u.]
m/z

Figure S11.

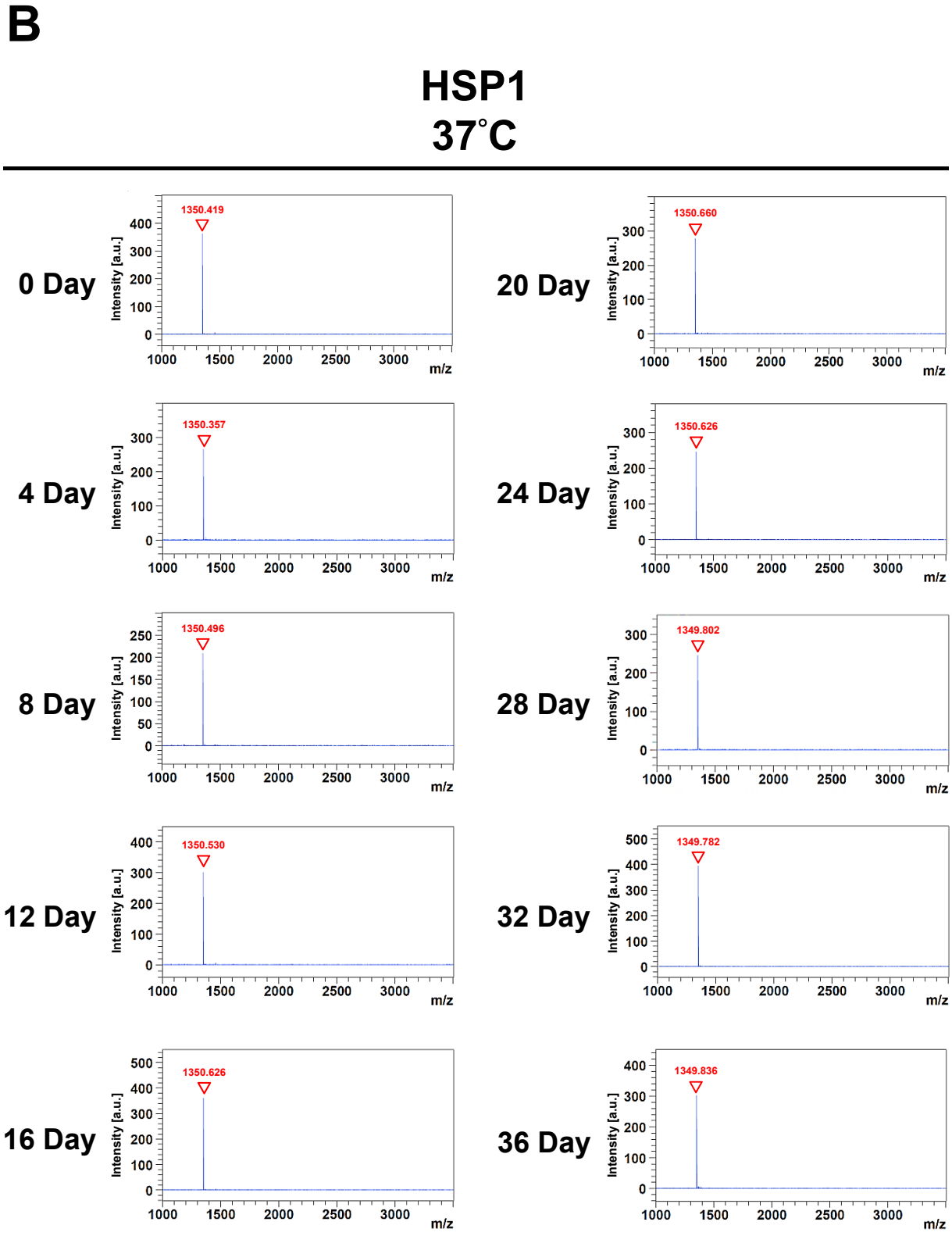
B
HSP1
37°C
0 Day
1350.419
4 Day
1350.357
8 Day
1350.496
12 Day
1350.530
16 Day
1350.626
20 Day
1350.660
24 Day
1350.626
28 Day
1349.802
32 Day
1349.782
36 Day
1349.836
Intensity [a.u.]
m/z

Figure S11.

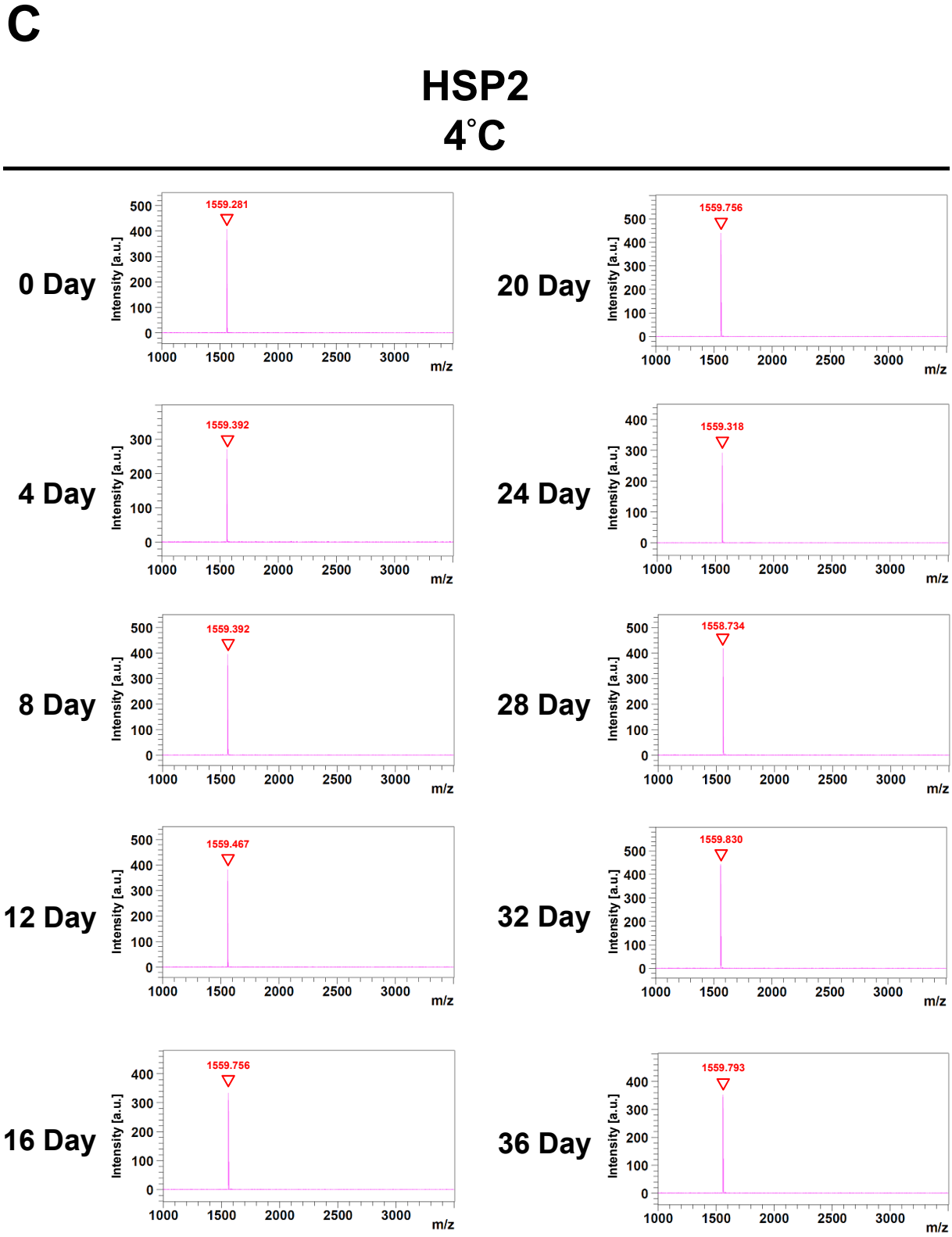
C
HSP2
4°C
0 Day
1559.281
20 Day
1559.756
4 Day
1559.392
24 Day
1559.318
8 Day
1559.392
28 Day
1558.734
12 Day
1559.467
32 Day
1559.830
16 Day
1559.756
36 Day
1559.793
Intensity [a.u.]
m/z

Figure S11.

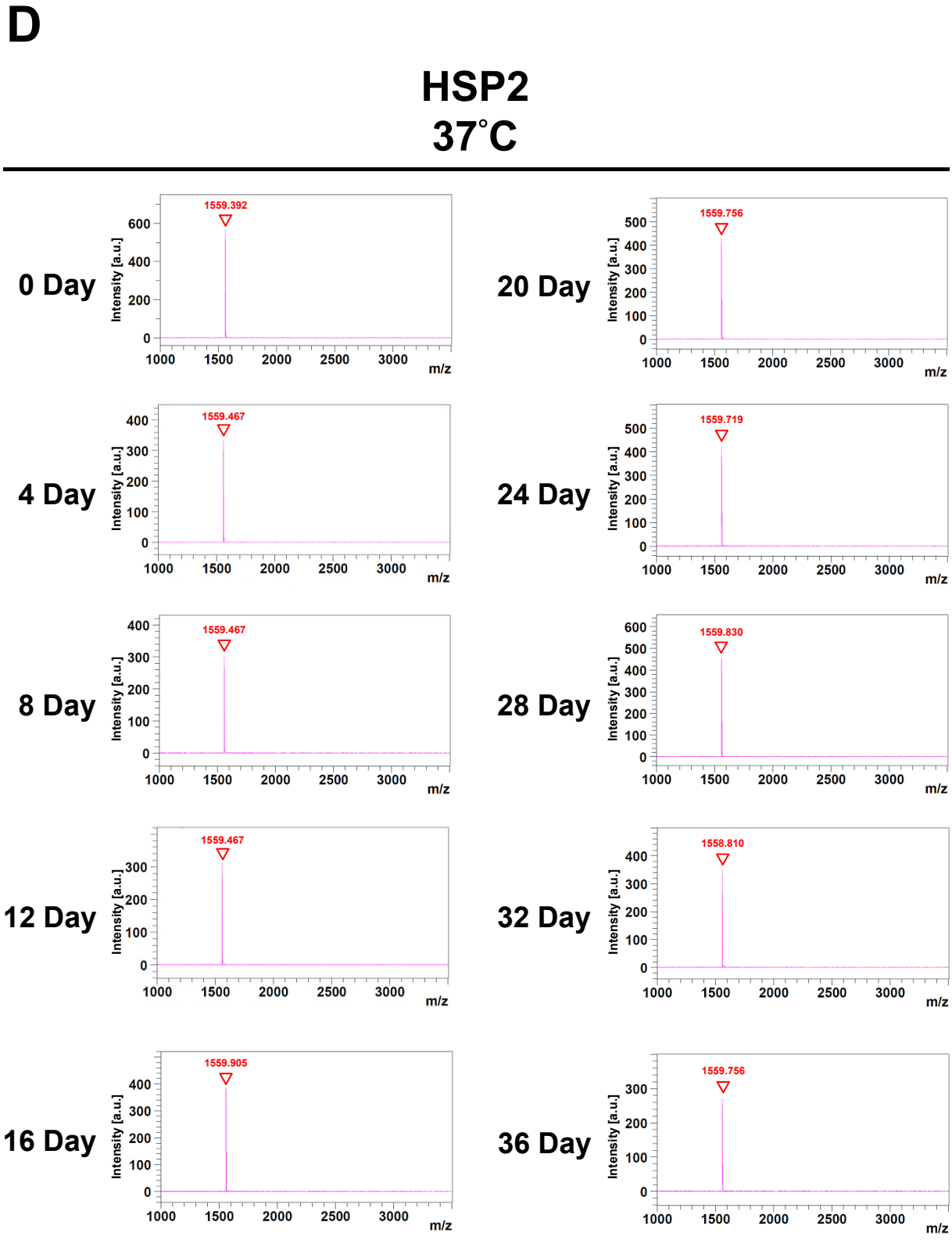
D
HSP2
37˚C
0 Day
1559.392
20 Day
1559.756
4 Day
1559.467
24 Day
1559.719
8 Day
1559.467
28 Day
1559.830
12 Day
1559.467
32 Day
1558.810
16 Day
1559.905
36 Day
1559.756
Intensity [a.u.]
m/z

Figure S11.

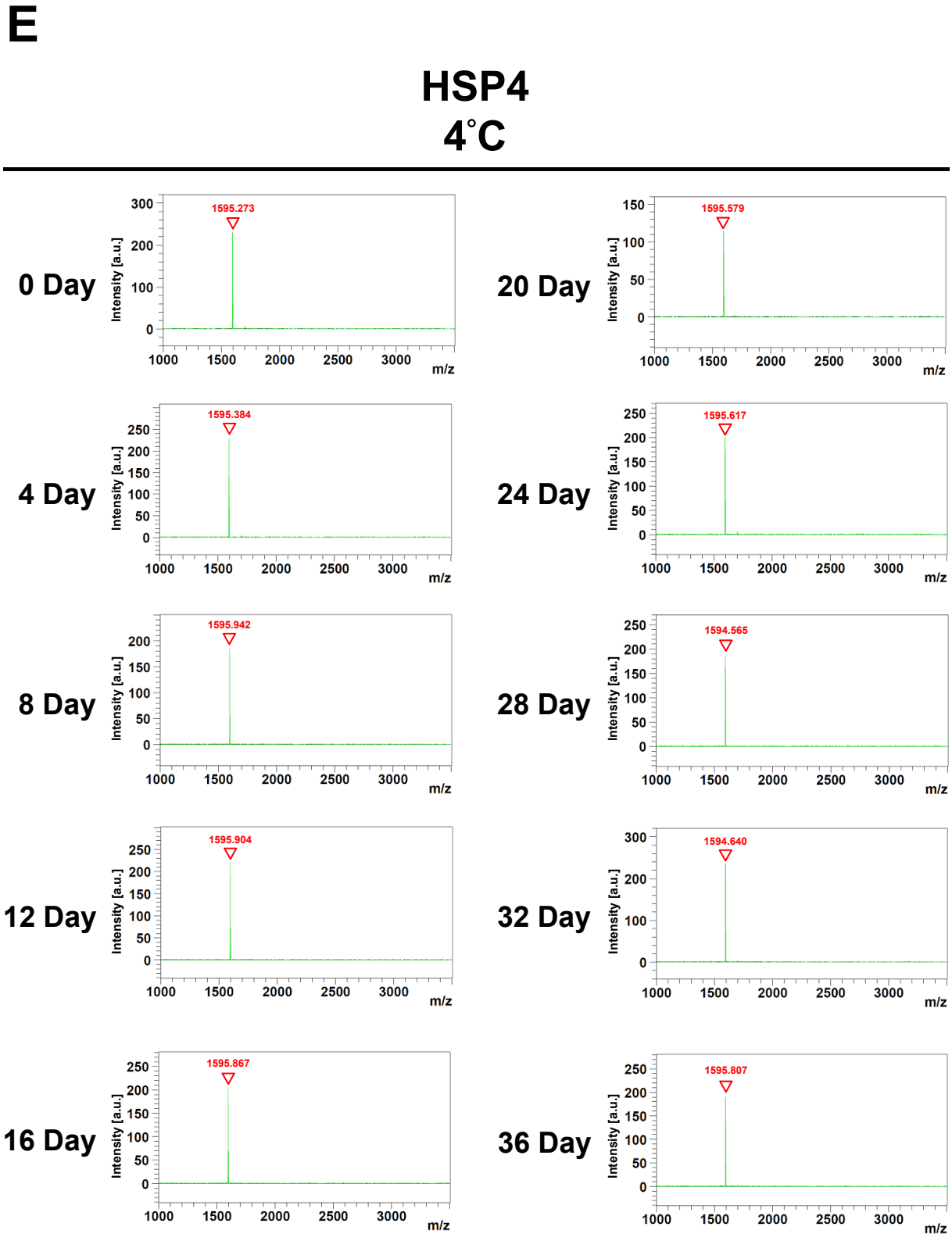
E
HSP4
4°C
0 Day
1595.273
20 Day
1595.579
4 Day
1595.384
24 Day
1595.617
8 Day
1595.942
28 Day
1594.565
12 Day
1595.904
32 Day
1594.640
16 Day
1595.867
36 Day
1595.807
Intensity [a.u.]
m/z

Figure S11.

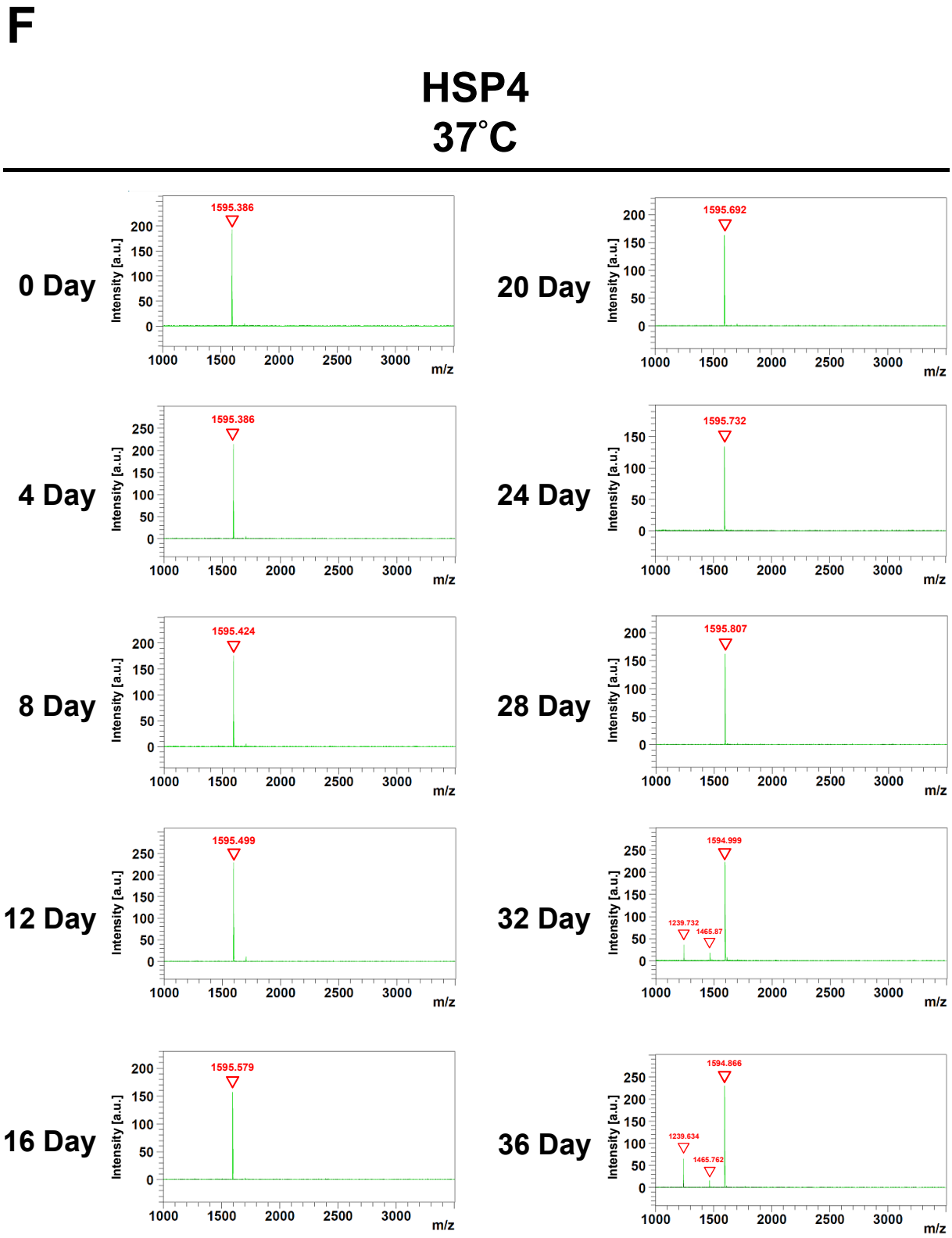
F
HSP4
37°C
0 Day
1595.386
4 Day
1595.386
8 Day
1595.424
12 Day
1595.499
16 Day
1595.579
20 Day
1595.692
24 Day
1595.732
28 Day
1595.807
32 Day
1594.999
1239.732
1465.87
36 Day
1594.866
1239.634
1465.762
Intensity [a.u.]
m/z

Figure S11.

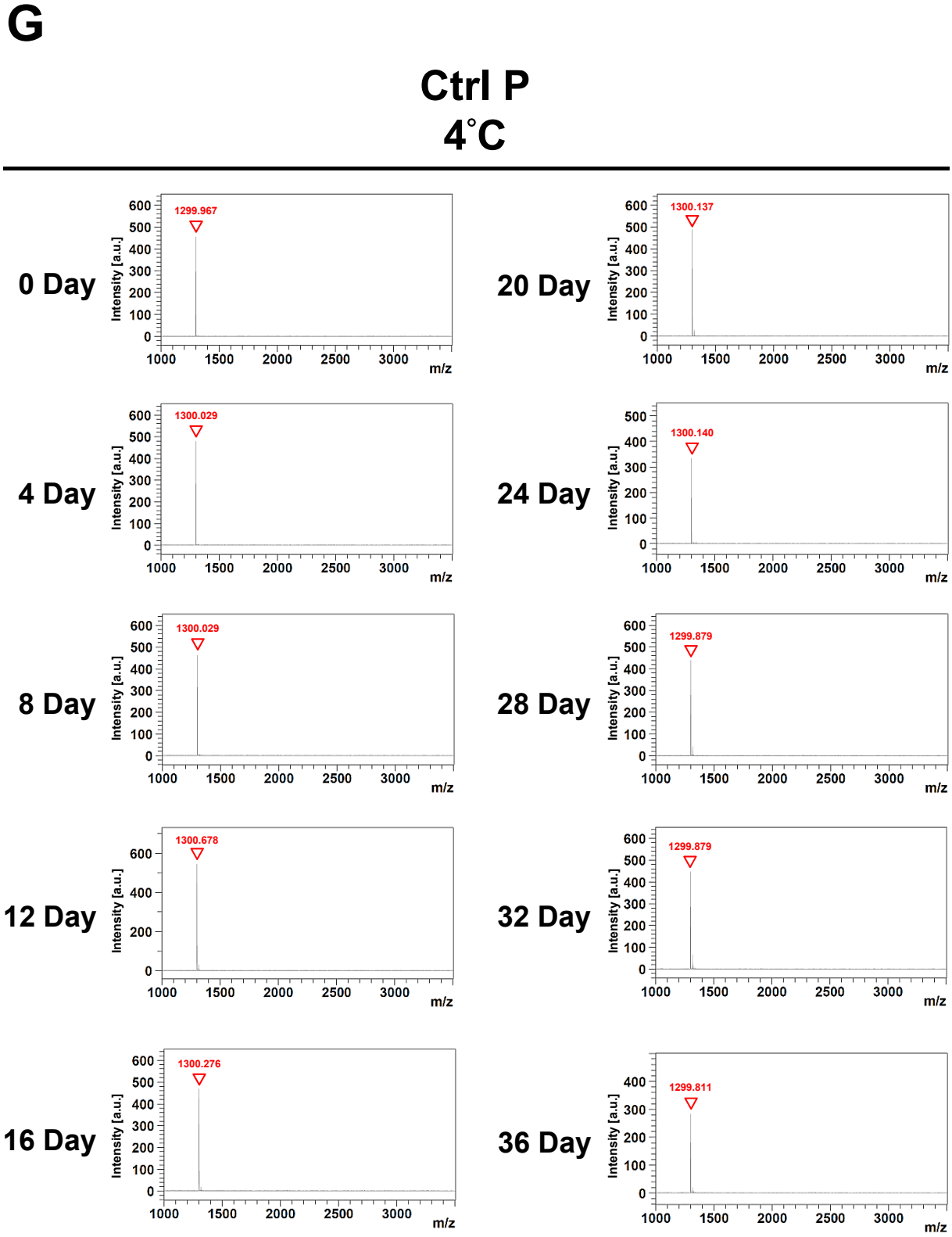
G
Ctrl P
4°C
0 Day
1299.967
20 Day
1300.137
4 Day
1300.029
24 Day
1300.140
8 Day
1300.029
28 Day
1299.879
12 Day
1300.678
32 Day
1299.879
16 Day
1300.276
36 Day
1299.811
Intensity [a.u.]
m/z

Figure S11.

H

Ctrl P
37°C

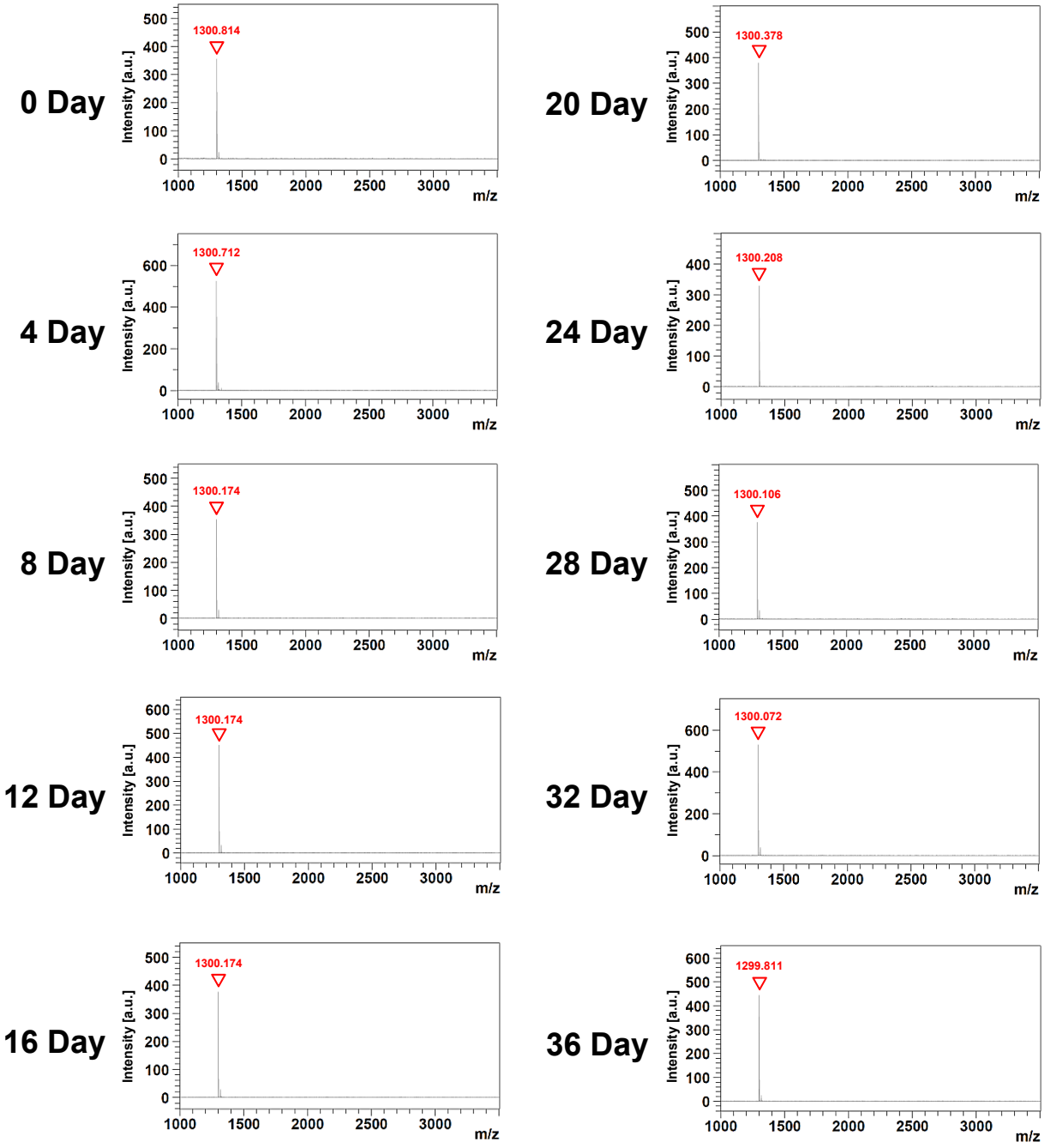

Figure S11. Peptide stabilities were measured by MALDI-TOF mass spectrometry.

HSP and control peptides were dissolved in water solution at 4°C and 37°C for 0, 4, 8, 12, 16, 20, 24, 28, 32, and 36 days, respectively. The molecular mass of the peptide polymers was measured by MALDI-TOF mass spectrometry at each time point. Except for HSP4, which was stable for only 28 days at 37°C and showed degraded peaks at 32 and 36 days (F), all other peptides were stable for at least 36 days at 4°C and 37°C (A-E, G-H).

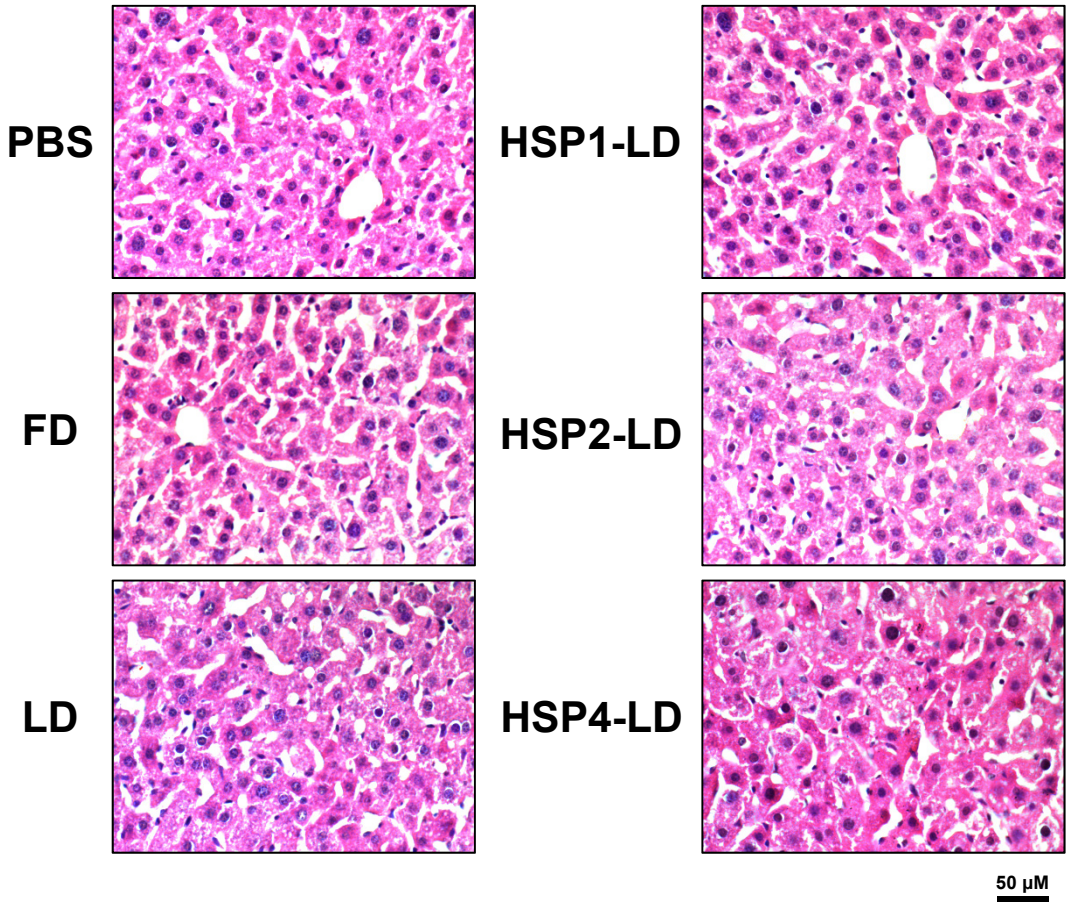

Figure S12. Hematoxylin and eosin staining of the liver tissues at 24 hr after a single dose of 2 mg/kg drug injection.

Mice liver tissues were collected from the biodistribution assay of Figure 6E at 24 hr post-injection. Hematoxylin and eosin staining showed that the liver toxicity was minimal in each group of liver tissues. Scale bar, 50 μm.

Figure S13.

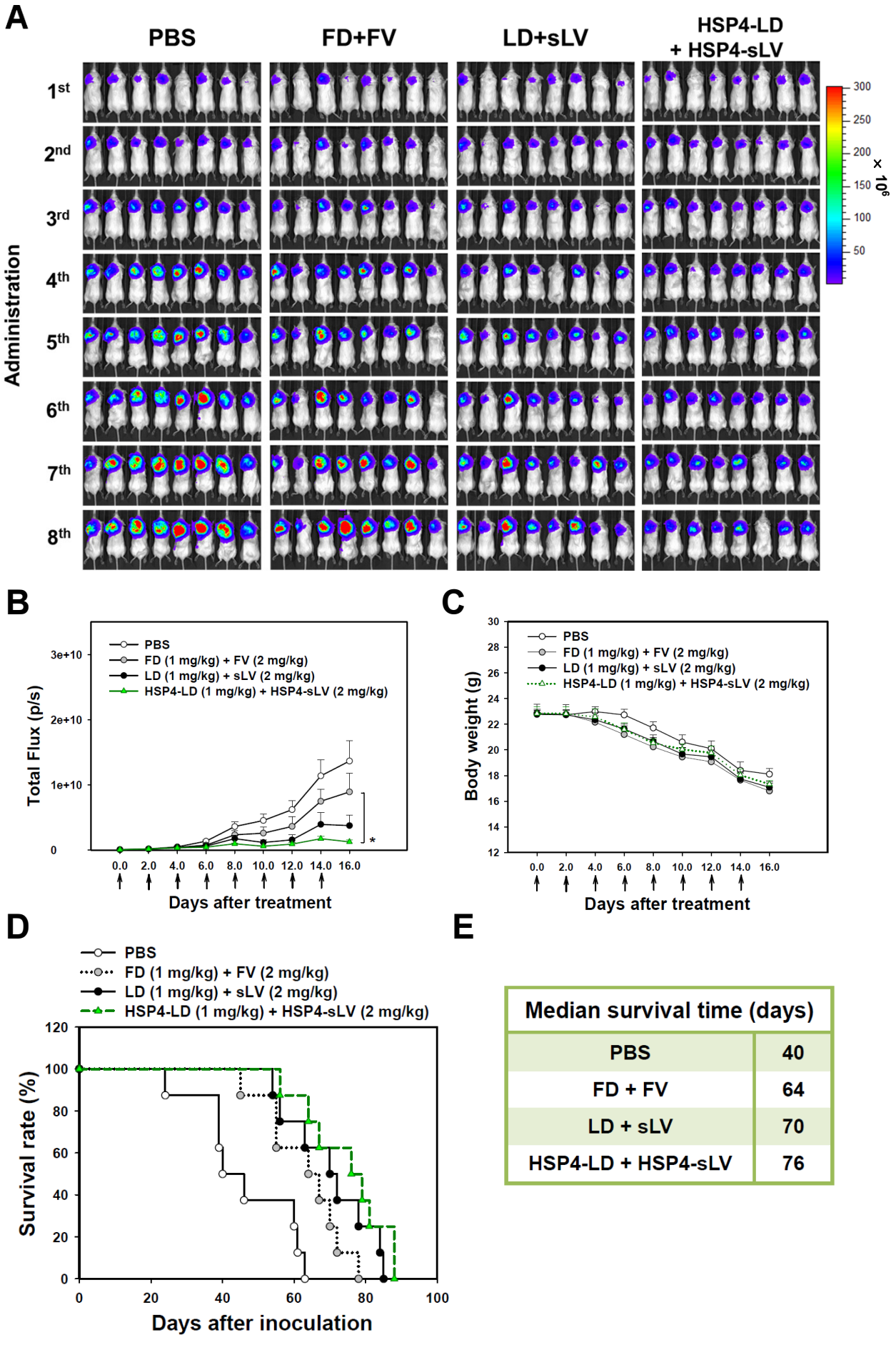

E

Median survival time (days)	
PBS	40
FD + FV	64
LD + sLV	70
HSP4-LD + HSP4-sLV	76

Figure S13. HSP4-LD and HSP4-sLV combination therapy in an orthotopic model of H460 LCC.

(A) Imaging drug response of mice with luciferase-expressing H460 cell transplants to combination therapy with FD/FV, LD/sLV, or HSP4-LD/HSP4-sLV at doses of 1/2 mpk, delivered by i.v. injection. Controls were treated with an equal volume of PBS. A total of 5 × 10^5 cells were transplanted with Matrigel, and treatment started 4 days after cancer cell transplantation (once every two days for 16 days). *n*=8 in each group. (B) Luminescence signals in tumor were quantified using IVIS200 software. *, $P<0.05$. (C) Body weight during the course of treatment. (D) Kaplan-Meier survival curve and (E) median survival time of recipient mice (HSP4-LD+HSP4-sLV vs. FD+FV; *, $P=0.0276$) (LD+sLV vs. FD+FV; no significance, $P=0.1808$).

Figure S14.

A

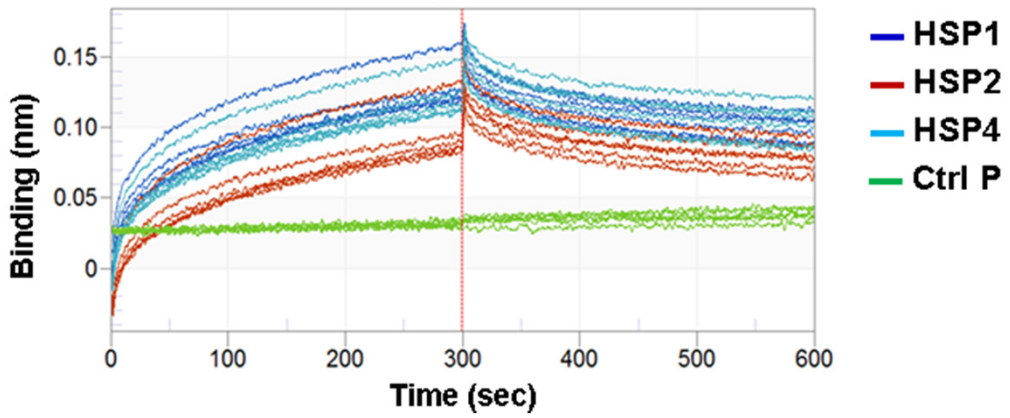

B

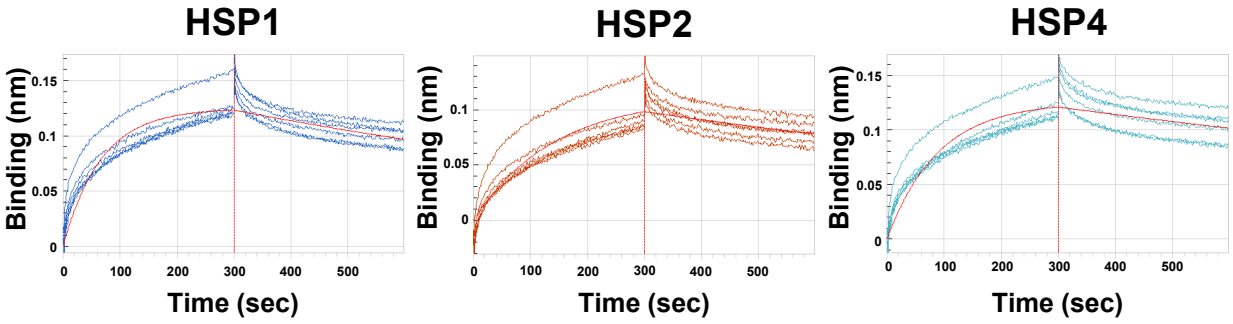

C

	H460 membrane extract		
	k_a ($M^{-1} \cdot s^{-1}$)	k_d (s^{-1})	K_D (M)
HSP1	1.41×10^{2}	8.09×10^{-4}	5.72×10^{-6}
HSP2	6.26×10^{1}	7.80×10^{-4}	1.25×10^{-5}
HSP4	1.06×10^{2}	5.83×10^{-4}	5.52×10^{-6}
Ctrl P	–	–	Weak binding

Dash (–) indicates no significant binding.

Figure S14. Binding affinity and kinetics between HSP peptides and H460 cell membrane extract determined by Bio-Layer Interferometry (BLI) assay.

(A-B) Representative sensorgrams of serial dilutions of HSP1, HSP2, and HSP4 binding to membrane components extracted from H460 cells. All sensorgrams were baseline-adjusted, and the H460 cell membrane extract was pre-subtracted with tag antibody to avoid non-specific binding. (A) HSP1, 2, 4, and Ctrl P with the same diluted concentrations were shown for comparison. (B) Separate sensorgrams of serial dilutions ranging from 5 to 200 μM and the optimal fitting curve (red line) for each peptide. The sensorgrams were measured by FortéBIO Octet® HTX system and fitted with FortéBIO Data Analysis Software version 9.0.0.10 to determine the association rates (k_a), dissociation rates (k_d), and equilibrium dissociation constants (K_D) as reported in (C).

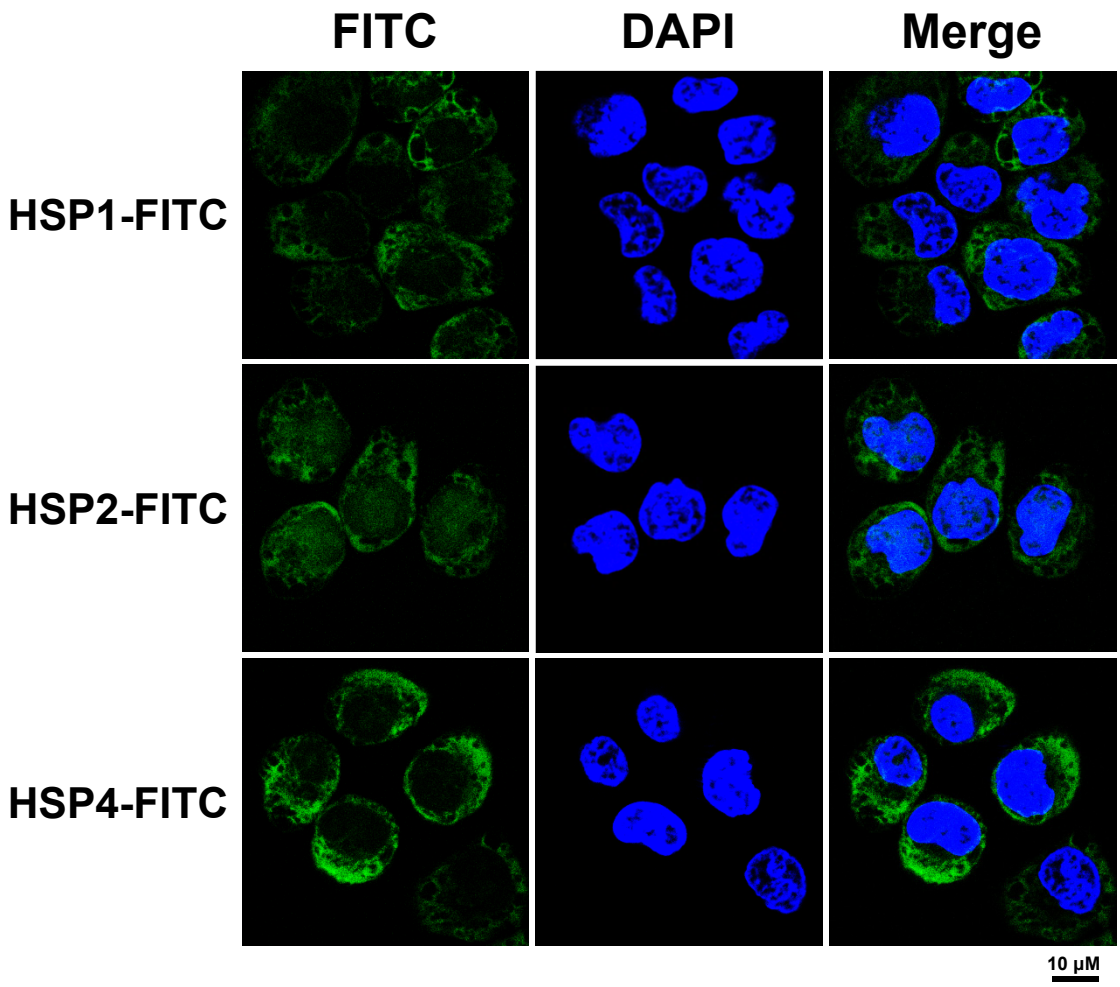

Figure S15. Target molecule localization of HSP peptides on H460 cells by confocal microscopy.

0.1% Triton X-100 permeabilized H460 cells were incubated with FITC-labeled HSP1, HSP2, and HSP4 peptides. The targets of HSP1, HSP2, and HSP4 were localized in the cell membrane and cytosol. The nuclei were stained with DAPI. Scale bar, 10 μm.

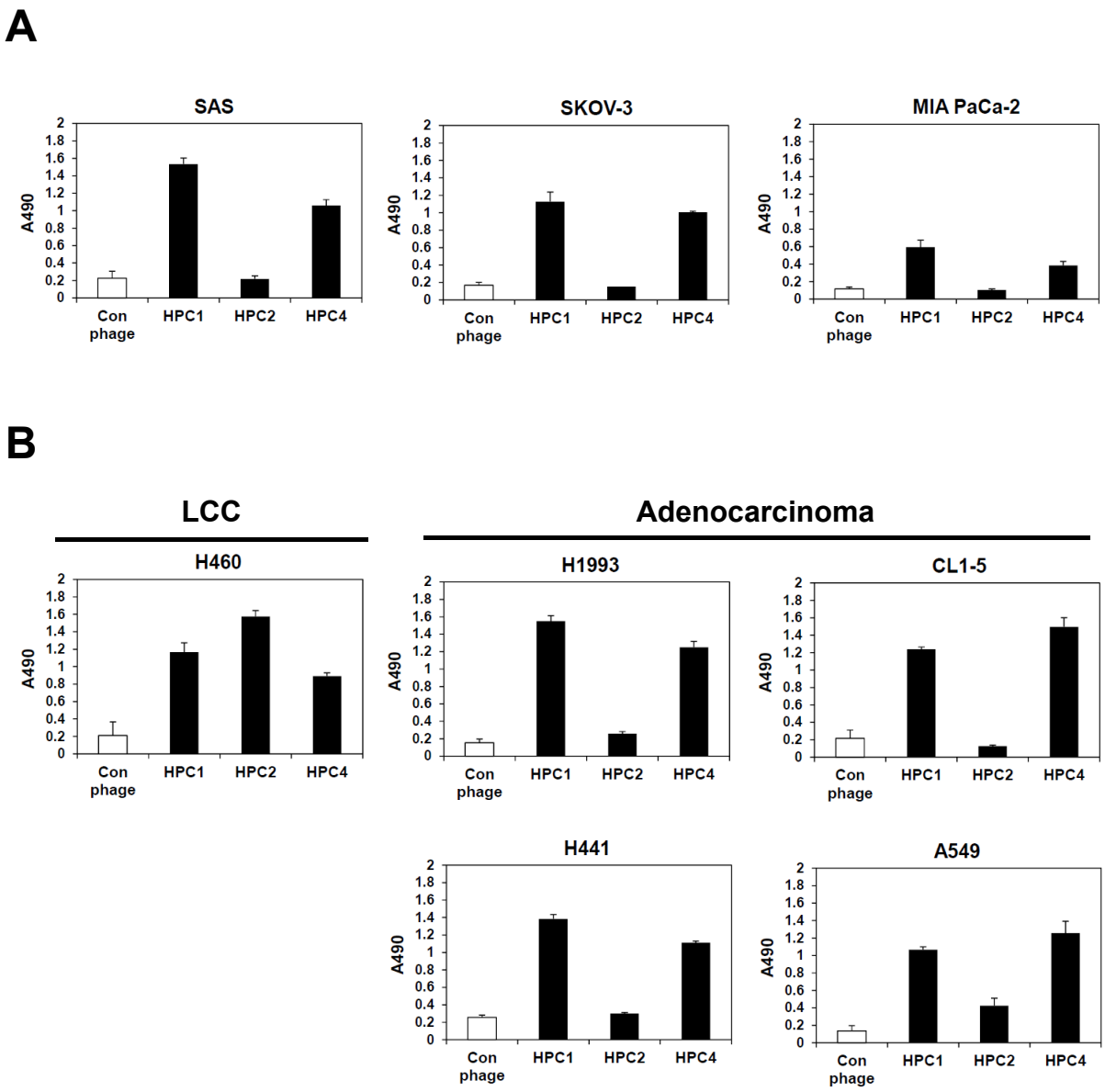

Figure S16. HPC1 and HPC4 can also bind to tongue SCC, ovarian adenocarcinoma, and pancreas ductal adenocarcinoma cell lines.

The binding intensities of HPC1, HPC2, HPC4, and control phage to other cancer types (A), lung LCC and lung adenocarcinoma (B) by ELISA of paraformaldehyde-fixed cells.